





Article

Apoptotic Induction in Human Cancer Cell Lines by Antimicrobial Compounds from Antarctic *Streptomyces fildesensis* (INACH3013)

David Astudillo-Barraza ¹, Romulo Oses ², Carlos Henríquez-Castillo ^{3,4}, Clemente Michael Vui Ling Wong ⁵ , José M. Pérez-Donoso ⁶ , Cristina Purcarea ⁷ , Heidge Fukumasu ⁸ , Natalia Fierro-Vásquez ⁹, Pablo A. Pérez ¹⁰ and Paris Lavin ^{9,11,*}

¹ Centro de Investigaciones Biomédicas (CIB), Escuela de Medicina, Universidad de Valparaíso, Av. Hontaneda N° 2664, Valparaíso 2340000, Chile

² Centro Regional de Investigación y Desarrollo Sustentable de Atacama (CRIDESAT), Universidad de Atacama, Av. Copayapu N° 485, Copiapó 1780000, Chile

³ Laboratorio de Fisiología y Genética Marina (FIGEMA), Departamento de Acuicultura, Facultad de Ciencias del Mar, Universidad Católica del Norte, Larrondo 1281, Coquimbo 1781421, Chile

⁴ Centro de Estudios Avanzados en Zonas Áridas (CEAZA), Larrondo 1281, Coquimbo 1781421, Chile

⁵ Biotechnology Research Institute, Universiti Malaysia Sabah, Jalan UMS, Kota Kinabalu 88400, Sabah, Malaysia

⁶ BioNanotechnology and Microbiology Laboratory, Center for Bioinformatics and Integrative Biology (CBIB), Faculty of Biological Sciences, Universidad Andres Bello, República 330, Santiago 8370146, Chile

⁷ Institute of Biology Bucharest of the Romanian Academy, 296 Splaiul Independentei, 060031 Bucharest, Romania

⁸ Department of Veterinary Medicine, Faculty of Animal Science and Food Engineering, University of São Paulo, Pirassununga 13635-105, SP, Brazil

⁹ Departamento de Biotecnología, Facultad de Ciencias del Mar y Recursos Biológicos, Universidad de Antofagasta, Antofagasta 1270300, Chile

¹⁰ Departamento de Ciencias Farmacéuticas, Facultad de Ciencias, Universidad Católica del Norte, Antofagasta 1240000, Chile

¹¹ Laboratorio de Complejidad Microbiana y Ecología Funcional, Instituto Antofagasta, Antofagasta 1240000, Chile

* Correspondence: paris.lavin@uantof.cl



Citation: Astudillo-Barraza, D.; Oses, R.; Henríquez-Castillo, C.; Vui Ling Wong, C.M.; Pérez-Donoso, J.M.; Purcarea, C.; Fukumasu, H.; Fierro-Vásquez, N.; Pérez, P.A.; Lavin, P. Apoptotic Induction in Human Cancer Cell Lines by Antimicrobial Compounds from Antarctic *Streptomyces fildesensis* (INACH3013). *Fermentation* **2023**, *9*, 129. <https://doi.org/10.3390/fermentation9020129>

Academic Editors: Nikos G. Chorianopoulos and Francesca Berini

Received: 20 December 2022

Revised: 7 January 2023

Accepted: 24 January 2023

Published: 29 January 2023



Copyright: © 2023 by the authors. Licensee MDPI, Basel, Switzerland. This article is an open access article distributed under the terms and conditions of the Creative Commons Attribution (CC BY) license (<https://creativecommons.org/licenses/by/4.0/>).

Abstract: The Antarctic *Streptomyces fildesensis* has been recognized for its production of antimicrobial compounds with interesting biological activities against foodborne bacteria and multi-resistant strains, but not for its potential antiproliferative activity and mechanisms involved. Two bioactive ethyl acetate extract (EAE) fractions were purified via thin-layer chromatography and High-Performance Liquid Chromatography (HPLC), showing that orange-colored compounds displayed antimicrobial activity against pathogenic bacteria even after shock thermal treatment. The UV–VIS features of the active compounds, the TLC assay with actinomycin-D pure standard, Fourier transform infrared (FTIR) spectra and the ANTISMASH analysis support the presence of actinomycin-like compounds. We demonstrated that *S. fildesensis* displays antiproliferative activity against human tumor cell lines, including human breast cancer (MCF-7), prostate cancer (PC-3), colon cancer (HT-29) and non-tumoral colon epithelial cells (CoN). The half-maximal effective concentrations (EC₅₀) ranged from 3.98 µg/mL to 0.1 µg/mL. Our results reveal that actinomycin-like compounds of *S. fildesensis* induced apoptosis mediated by caspase activation, decreasing the mitochondrial membrane potential and altering the cell morphology in all tumoral and non-tumoral cell lines analyzed. These findings confirm the potential of the psychrotolerant Antarctic *S. fildesensis* species as a promising source for obtaining potential novel anticancer compounds.

Keywords: *Streptomyces fildesensis*; cytotoxic; antimicrobial; anticancer; apoptosis; mitochondrial membrane permeability; caspases

1. Introduction

Cancer and multi-resistant pathogens are a major global health problem [1]. Prostate, colorectal and breast cancers are the most common diagnosed cancers in the world [1]. Finding new antibiotics and effective anticancer drugs is a major research focus.

The genus *Streptomyces* has attracted significant interest due to its ability to synthesize different biologically active secondary metabolites, including more than 80% of known antibiotics, antitumoral molecules and growth effectors, among other compounds. Consequently, the genus *Streptomyces* is considered a primary source of useful drugs to improve human life that cannot be matched by any other organism [2,3]. These bioactive compounds are mainly produced by the activation of cryptic gene clusters that are not active under normal conditions [4]. Microorganisms that inhabit extreme environments have evolved to cope with abiotic stresses in their environment, offering huge potential for the discovery of bioactive compounds. In this sense, the *Streptomyces* species, derived from extreme sources, is still an extraordinary reservoir of novel biosynthetic gene clusters with the potential for developing anticancer drugs [5].

Despite efforts to explore the biotechnological potential of polar streptomycetes, there is still very little information regarding its chemical characteristics and potential bioactivity. Recently, two psychrotrophic Antarctic *Streptomyces fildesensis* strains (INACH3013 and So13.3) have been reported to inhibit the growth of several pathogens, including the food-borne pathogens *Staphylococcus aureus* ATCC 25923 and MRSA [6,7]. The *S. fildesensis* strain So13.3 contains biosynthetic gene clusters [BGCs] for the synthesis of diverse antibiotics, including streptorubin, surfactin, sarmentoside, prenyletin, dactinomycin, actinomycin and piericidin [7]. A previous report described the presence of an actinomycin-D-related analog in the crude extract of phylogenetically related *S. fildesensis*. This extract shows pronounced antiproliferative activity in tumor cell lines [8].

Actinomycin is a class of chromopeptide lactone antibiotics produced by several species of *Streptomyces*. Among the 30 different molecules described, actinomycin D is one of the most studied molecules and is widely used for tumor treatment [9,10]. Its anticancer role has been associated with the inhibition of RNA Polymerase I (RNA Pol I) due to its ability to intercalate double-stranded DNA, blocking ribosome biogenesis and inducing nucleolar stress response [10,11]. Despite current actinomycin studies, there are still some knowledge gaps regarding its chemical structure and its relationship with antitumoral action mechanisms, which are very important aspects to understand in deep biological activities.

The production of bioactive compounds in Antarctic *Streptomyces* requires exploring not only new strains but also experimental procedures to pose Antarctic streptomycetes as a source of novel compounds. With this in mind, the present work aimed to characterize the activity of two major purified fractions present in the cell-free supernatant of the *Streptomyces fildesensis* strain INACH3013 against different human cancer cell lines. Based on these results, the putative mechanisms involved in apoptosis, as well as the potential application of these bioactive compounds, are discussed.

2. Materials and Methods

2.1. *Streptomyces fildesensis* INACH3013 Growth Conditions and Extracts

The psychrotrophic *S. fildesensis* INACH3013, isolated from soil of the Antarctic Fildes Peninsula (62°12'26.4" S, 58°58'28.7" W) [6], was grown in triplicate in 200 mL of Oatmeal medium (30 g/L) at 12 °C with shaking (180 rpm) for 5 days [12]. Cell-free supernatants (CFS) were obtained by centrifuging the cultures at 8000 × g for 10 min. Secondary metabolites were extracted from the CFS by using ethyl acetate 1:1 (v/v) as described previously [13]. The CFS and ethyl acetate extract (EAE) were lyophilized and stored at −20 °C until use.

2.2. Thin-Layer Chromatography Direct Bioautography (TLC)

Thin-layer chromatography (TLC) was performed to separate and screen the most active compounds through the bioautography detection method [14]. Samples of 10 μL of EAE (45 μg) were loaded in triplicate onto TLC plates and were developed with a mixture of ethyl acetate and methanol (9:1 *v/v*) as the mobile phase. After drying, the compound spots were visualized under visible and short UV (366 nm) light. Ten spots were cut, eluted and used for further assay against *Staphylococcus aureus* ATCC 6538P. The strain was grown in 1.3% Mueller–Hinton (MH) broth at 37 °C for 6 h and was grown in molten MH agar up to an OD₆₀₀ of 0.001. The molten agar was further poured into an empty petri dish with spots and was allowed to solidify. The inhibition zones (mm²) were visualized after incubation at 37 °C for 24 h. The inhibition zone was used as an indicator of the antimicrobial activity associated with each spot. The two major colored spots with remarkable activity (retention factor = $R_f = 0.65$ and $R_f = 0.72$) were chosen and processed for purification. Authentic actinomycin D (Thermo Fisher, Grand Island, NY, USA) was used as the standard to perform one-dimensional TLC (1D-TLC; Figure 1H) and two-dimensional TLC (2D-TLC; Figure S1).

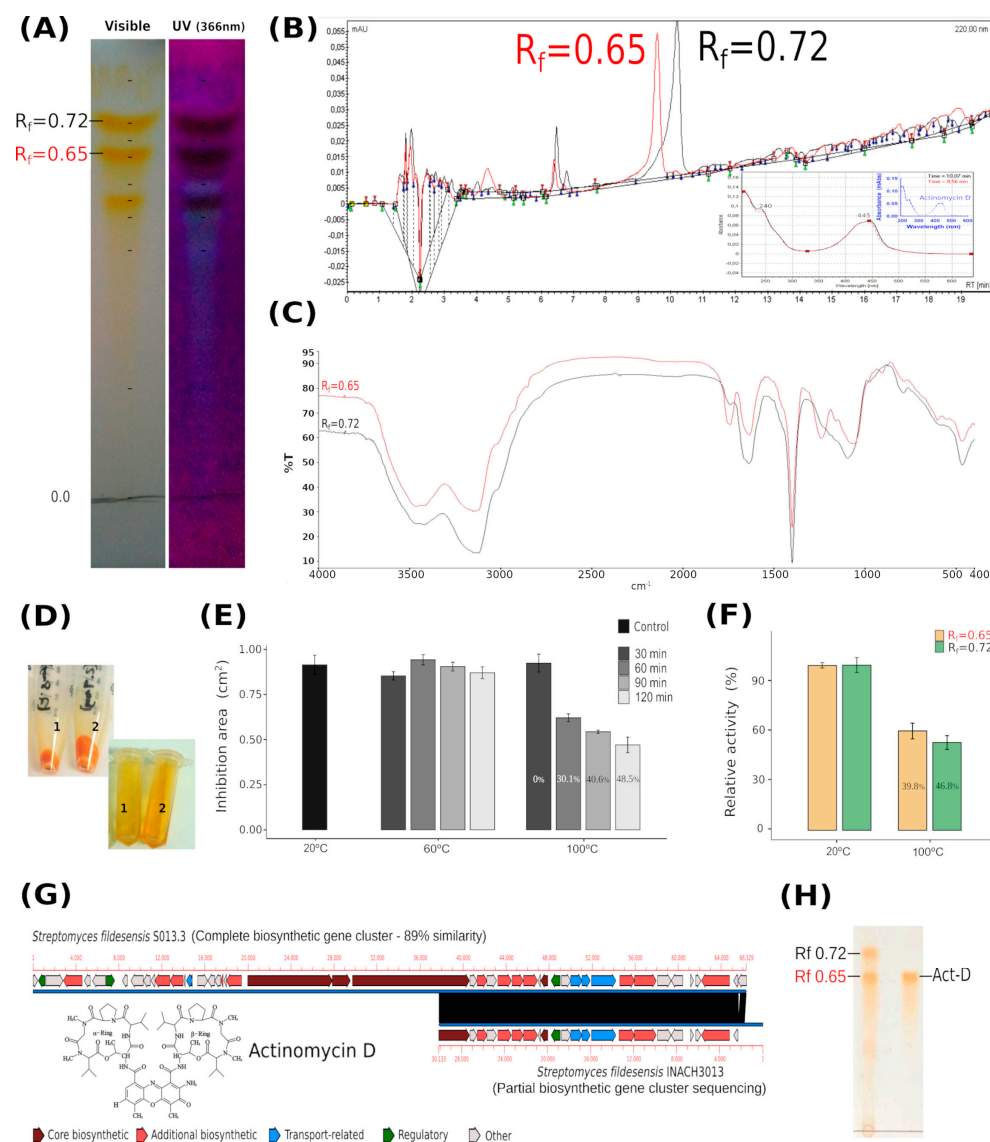


Figure 1. Separation, purification and thermal stability assay of extracellular fractions: (A) Thin-layer chromatography unstained fractions resulting from 45 μg EAE visualized in visible and UV light (ethyl acetate: methanol (9:1) used as the mobile solvent); (B) HPLC analysis of $R_f = 0.65$ and $R_f = 0.72$ samples obtained from TLC and UV–visible spectra of the $R_f = 0.65$ (red) and $R_f = 0.72$ (black) fractions

compared with typical spectra of actinomycin D (blue—figure modified from Lee et al. 2016); (C) FTIR spectrum of isolated Actinomycin; (D) Color of purified $R_f = 0.65$ (1) and $R_f = 0.72$ (2) fractions lyophilized (orange) and in acetonitrile (yellow); (E) Thermal stability of EAE antibacterial activity after exposure to 20 °C, 60 °C and 100 °C for different times (0, 30, 60, 90, 120 min); (F) Thermal stability of the two pigmented isolated fractions. The relative antibacterial activity of the major TLC fractions was expressed as the percentage of activity loss after 1 h of thermal treatment as compared to that of the control at 20 °C; (G) Biosynthetic cluster involved in the actinomycin production of *S. fildesensis* strain So13.3 and synteny analysis on strain INACH3013; (H) TLC of EAE and actinomycin D.

2.3. Purification and Partial Characterization by High-Performance Liquid Chromatography (HPLC)

TLC spots with remarkable antimicrobial activity ($R_f = 0.65$ and $R_f = 0.72$) were resuspended in 60% acetonitrile. The separations and analysis of each spot's main compounds were performed via high-performance liquid chromatography (HPLC) using a Jasco PU 980 (Spectroscopic Tokyo, Japan) provided with a UV detector (Jasco UV-970), an integrator (Jasco 807-IT) and a reverse phase column, Kromasil (100-5c18 250 × 4.6 mm). Fraction separation was performed in the gradient mobile phase (acetonitrile, ACN): ultra-pure water, acidified with trifluoroacetic acid (0.1% v/v) from 60% ACN to 85% ACN at a flow rate of 1 mg/mL. The volume of the injected sample was 100 µL, and the running time was 20 min. The absorption spectrum of the resulting fractions was analyzed in the UV-visible range (200–650 nm). The purified HPLC fractions were lyophilized for further analyses (thermal stability, cell viability assay, caspase activity and mitochondrial membrane potential).

2.4. FTIR Characterization

Fourier-transform infrared (FTIR) spectra for the characterization of the purified HPLC compounds obtained in this work were recorded in the spectral range of 4000–400 cm^{-1} (using KBr as reference) using a Perkin Elmer Frontier spectrophotometer (Perkin Elmer, Waltham, MA, USA).

2.5. Thermal Stability Assay in Bioactive Compounds

The thermal stability of compounds at different temperatures (20, 60 and 100 °C) and exposure times (30, 60, 90 and 120 min) was evaluated using a SmartBlock DWP 1000 Thermoblock (Eppendorf Ltd., Stevenage, UK). Lyophilized ethyl acetate extracts were resuspended in ethanol (1×) and diluted in water (100×) up to a final concentration of 5.7 mg/mL, and the aqueous solutions (10 µL) were inoculated over a molten agar medium seeded with *S. aureus* to evaluate the thermal response based on the produced inhibition halo [6]. Furthermore, purified HPLC fractions were incubated at 20 and 100 °C for 1 h, and the thermal stability was further determined in triplicate following the procedure described above. Due to different concentrations recovered from each spot, the results are expressed as the relative percentage of inhibition relative to the corresponding control at 20 °C.

2.6. Identifying Biosynthetic Gene Clusters (BGCs)

The presence of actinomycin-like secondary metabolite biosynthetic gene clusters was determined using AntiSMASH 5.0. (<https://antismash.secondarymetabolites.org/>, accessed on 1 April 2021) using strict parameters with all features selected [15]. This result was compared with the complete genome of the sister strain, So13.3. The BLAST-based (ANIb) and MUMmer-based (ANIm) whole-genome average nucleotide identity between strains was calculated with JspeciesWS [16]. In silico DNA–DNA hybridization (isDDH, GLM-based) was calculated with the genome-to-genome distance calculator (GGDC) [17]. Synteny analysis and the visualization of the main BGCs between both genomes of *S. fildesensis* strains, So13.3 [7] and INACH3013 [18], were performed with

TREBOL software (www.inf.imo-chile.cl/software/trebol.html accessed on 1 April 2021), using DC-MEGABLAST with an e value cut-off < 0.0001.

2.7. Cell Viability and Cytotoxicity Assay against Cancer Cell Lines

The cell lines used for the viability and cytotoxicity assay were human breast cancer (MCF-7), prostate cancer (PC-3), colon cancer (HT-29) and non-tumoral colon epithelial (CCD841) CoN. The cell lines were maintained at 37 °C in Ham's-F12: DMEM High Glucose medium (Gibco, San Diego, CA, USA) and were supplemented with 10% (*v/v*) fetal bovine serum (FBS), 100 U/mL penicillin, 100 µg/mL streptomycin and 1 mM glutamine in a humidified 5% CO₂ incubator. Serial dilutions of the extracts (CFS and EAE), as well as the purified HPLC fractions ($R_f = 0.65$ and $R_f = 0.72$), were prepared to achieve final concentrations ranging from 500 µg/mL to 0.0125 µg/mL. Cells were seeded in 96-well plates at 3×10^3 cells per well, containing the serial dilutions of each extract or fraction, and were then incubated in replicates ($n = 5$ per treatment) for 24 h. Cell viability was determined via the Sulforhodamine B (SRB) (Sigma, St. Louis, MO, USA) dye assay [19]. For this, cell lines were seeded at a density of 3×10^3 cells per well and were incubated for 24 h in 96-well plates. Then, cells were treated with CFS, EAE, $R_f = 0.65$ and $R_f = 0.72$ extracts for 24 h. After the treatment, cells were fixed by the addition of 25 µL of cold 50% (wt/vol) trichloroacetic acid and were incubated for 60 min at 4 °C. Then, plates were washed with deionized water and dried for 24 h. An amount of 50 µL of SRB solution (0.1% wt/vol in 1% acetic acid) was added to each well and incubated for 30 min at room temperature. Unbound SRB was removed by washing with 1% acetic acid. Plates were air-dried, and bounded staining was solubilized with 100 µL of Tris base (10 mM). Optical densities were read in an automated spectrophotometer plate reader at 540 nm. Finally, the percentage of cell viability and half-maximal effective concentration (EC₅₀) was determined. For the EC₅₀ calculation, the percentages were plotted against the logarithm of extract concentrations.

2.8. Morphological Characterization of Cell Apoptosis

Changes in cell morphology were analyzed using an inverted microscope (Olympus IX81, Olympus America, Center Valley, PA, USA). Morphological changes in the nuclear chromatin of cells undergoing apoptosis were evaluated using Hoechst 33342 nuclear fluorescent dye [20,21]. An amount of 1×10^4 cells/mL of CoN, HT-29, PC-3 and MCF-7 cell lines were seeded independently in 24-well plates and exposed to the selected compounds for 24 h; then, 1 µM of Hoechst 33342 was added to each well and incubated for 30 min in the dark at room temperature. The cells were further washed with cold phosphate-buffered saline (PBS), and cell viability was determined with the number of blue fluorescent cells as a proxy of the dye incorporation using a fluorescence microscope (Olympus IX81).

2.9. Analysis of Mitochondrial Membrane Potential (MMP)

Rhodamine 123 (Thermo Fisher Scientific), a cationic voltage-sensitive probe that reversibly accumulates in mitochondria, was used to detect changes in transmembrane MMP. CoN, PC-3 and HT-29 cell lines were seeded in 24-well plates (8×10^4 cells per well). Exponentially growing cells were incubated with EAE, $R_f = 0.65$ and $R_f = 0.72$ for 12, 24 and 48 h. Cells were stained with 1 mM of rhodamine 123 at 37 °C for 60 min. Cells were detached from the plate and washed with ice-cold PBS. Samples were analyzed via flow cytometry (BD FACSJazz™ Cell Sorter) using a 488 nm laser and by collecting the fluorescence at 585 nm. Data are expressed as the percentage of cells that were positive for rhodamine 123 dye.

2.10. Analysis of Caspase Activity

Caspase activity was determined using the fluorescent inhibitor of caspases tagged with fluorescein isothiocyanate, FITC-VAD-FMK (CaspACE™ FITC VAD-FMK In Situ Marker, Promega, Madison, WI, USA) according to the recommended manufacturer in-

structions. Flow cytometry was performed to measure the activity of total caspases [22,23]. Briefly, CoN, PC-3 and HT-29 cell lines were exposed to EAE, $R_f = 0.65$ and $R_f = 0.72$ fractions for 48 h. Cells were incubated with CaspACE™ in the dark for 20 min at room temperature. Subsequently, the medium was removed, and cells were washed twice with PBS. Exposed cells were collected via trypsinization and centrifugation (7 min at $1500 \times g$). The supernatant was discarded, and the pellet was resuspended in PBS and analyzed via flow cytometry using the 488 nm excitation laser and by collecting the fluorescence at 692 nm. The results of caspase activity are expressed as the times of induction in comparison with the control treatment.

2.11. Statistical Analyses

Statistics were performed using R v3.6.3 [24]. Statistical differences among treatments were evaluated using t-tests or one-way and two-way ANOVAs, followed by Tukey's HSD (honestly significant difference) test for multiple comparisons using the dplyr package [25]. A regression analysis was used to determine EC_{50} values using the tidyverse, ggplot2 and drc packages [26–28].

3. Results

3.1. Purification and Characterization of $R_f = 0.65$ and $R_f = 0.72$ Fractions by HPLC

The $R_f = 0.65$ and $R_f = 0.72$ fractions with antimicrobial activity were purified and characterized (Figure 1). The lyophilized extracts appeared as an orange-yellow powder. Both fractions turned from yellow to red when reacting with 20% sulfuric acid, and no reaction with 0.1% ninhydrin in ethanol was observed. Absorption spectra in the UV–visible range (220–500 nm) of both fractions revealed two peaks at 240 nm and 445 nm for both extracts (Figure 1B). The ratios of the absorbance at 240 nm to that at 445 nm were 1.3 and 1.35 for $R_f = 0.65$ and $R_f = 0.72$, respectively. When TLC was performed using actinomycin D as a reference, it exhibited the same R_f found for the $R_f = 0.65$ fraction (Figure 1H).

3.2. Thermal Stability of Bioactive Compound from *S. fildesensis* INACH3013

Streptomycete EAE was highly stable because exposure to 60 °C for 120 min did not induce a significant decrease in antimicrobial activity (Figure 1E; one-way ANOVA, $F(4,10) = 1.20$, $p = 0.254$). In the same way, no antimicrobial activity decrease was observed when the EAE was exposed to 100 °C for 30 min (Figure 1E).

However, the antimicrobial activity of the EAE decreased to 48.5% after 120 min of incubation at 100 °C (Figure 1E; one-way ANOVA, $F(4,10) = 29.2$, $p < 0.001$). Regarding the purified fractions, the reduction in antibacterial activity with the high-temperature treatment (100 °C for one hour) was significant for the analyzed fractions (one-way ANOVA, $F(3,8.37) = 35.7$, $p < 0.001$). The observed loss of activity after the 1 h treatment ranged between 46.8% and 39.8%, which correlates with the degree of polarity of each fraction ($R_f = 0.72 > R_f = 0.65$), with the non-polar fraction being more sensitive to temperature (Figure 1F). No significant differences among the fractions in terms of antimicrobial activity was observed (Student's $df = 8$, $p = 0.302$; Figure 1F).

3.3. Identification of Secondary Metabolite Biosynthetic Gene Clusters

The strain INACH3013 harbors 33 gene clusters for the biosynthesis of secondary metabolites (Table S1), including genes for the potential production of antibiotics such as actinomycin. Other BGCs with high similarity to well-known BGCs corresponded to ectoine, melanin, geosmin, alkylresorcinol, spore pigment, pristinol and hopene, with gene similarities to known BGCs ranging from 73% to 100%. For the BGCs in *S. fildesensis* So13.3, 29 secondary metabolite regions were found in this sister strain (Table S1).

3.4. Cytotoxic Effect of Bioactive Compounds from *S. fildesensis* INACH3013

The CFS, EAE extract and TLC purified fractions ($R_f = 0.65$ and $R_f = 0.72$) exerted differential cytotoxicity against a series of challenged cancer cell lines (Table 1). The CFS exerted the least cytotoxic effect among all the tested cell lines.

Table 1. Cytotoxicity of *Streptomyces* extracts and fraction. The half-maximal effective concentration (EC_{50}) values of the cell-free supernatant (CFS), ethyl acetate extracts (EAE) and the $R_f = 0.65$ and $R_f = 0.72$ fractions recovered from TLC spots against MCF-7, PC-3 and HT-29 cells and from non-tumoral colon epithelial cells CCD841 (CoN) used as the control were calculated as described in Materials and Methods as the mean \pm standard error of the mean (SEM), $n = 5$.

Sample	EC_{50} ($\mu\text{g/mL}$)			
	CoN F = 58.13; $p < 0.0001$	MFC-7 F = 37.95; $p < 0.0001$	PC-3 F = 14.25; $p < 0.0001$	HT-29 F = 43.42; $p < 0.0001$
CFS $F = 0.3557$; $p = 0.8738$	17.52 \pm 2.18 <i>g,h,i</i>	12.97 \pm 1.99 <i>j,l,m</i>	11.95 \pm 2.84 <i>n,o</i>	13.42 \pm 1.96 <i>r,s,t</i>
EAE $F = 6.953$; $p < 0.0001$	0.49 \pm 0.14 ^{d,f}	0.06 \pm 0.01 ^d	0.35 \pm 0.04	0.10 \pm 0.02 ^f
$R_f = 0.65$ $F = 25.97$; $p < 0.0001$	1.50 \pm 0.28 ^a	2.04 \pm 0.19 ^b	7.71 \pm 1.13 ^{a,b,c}	1.16 \pm 0.25 ^c
$R_f = 0.72$ $F = 5.335$; $p = 0.0097$	0.16 \pm 0.02 <i>i</i>	0.14 \pm 0.01 <i>m</i>	0.19 \pm 0.01 ^e <i>o,q</i>	0.09 \pm 0.01 ^e <i>t</i>

(One-way ANOVA with post hoc Tukey’s HSD test by row: ^{a,b,c} $p < 0.001$; ^{d,e} $p < 0.01$; ^f $p < 0.05$; by column: *g, h, i, j, l, m, n, o, r, s, t* $p < 0.001$; *p, q* $p < 0.05$).

Higher cytotoxic activity was achieved by both the EAE and the $R_f = 0.72$ fraction. Independently from the cellular line assayed, the cytotoxicity of the $R_f = 0.72$ fraction was significantly higher than the cytotoxicity of the $R_f = 0.65$ fraction, ranging between 9 and 40 times higher. As Table 2 shows, the cytotoxicity of the $R_f = 0.72$ fraction (measured as EC_{50}) was significantly higher than the cytotoxicity found in the total EAE for all cellular lines except MFC-7.

Table 2. Effect of metabolites on the mitochondrial membrane potential (MMP). Percentage of cells labeled with rhodamine 123 after treatment with total ethyl acetate extract (EAE), fraction $R_f = 0.65$ and fraction $R_f = 0.72$ for 12 h, 24 h and 48 h (mean \pm standard deviation; $n = 5$).

Treatments	Mitochondrial Membrane Potential (%)			
		Cell Lines		
		CoN	PC-3	HT-29
EAE	12 h	69.6 \pm 0.61	34.3 \pm 0.52	26.0 \pm 0.47
	24 h	48.1 \pm 0.31	34.4 \pm 0.67	30.6 \pm 0.75
	48 h	32.1 \pm 0.34	46.9 \pm 0.97	62.1 \pm 3.21
$R_f = 0.65$	12 h	63.2 \pm 0.54	35.9 \pm 1.30	26.4 \pm 0.70
	24 h	36.4 \pm 0.32	81.0 \pm 1.36	82.6 \pm 0.12
	48 h	15.6 \pm 1.15	91.3 \pm 4.17	98.8 \pm 0.15
$R_f = 0.72$	12 h	21.2 \pm 0.90	44.7 \pm 1.16	37.5 \pm 0.24
	24 h	20.2 \pm 1.37	43.6 \pm 0.48	28.0 \pm 0.28
	48 h	22.8 \pm 0.69	36.1 \pm 0.15	24.0 \pm 0.13
Two-way ANOVA (treatment vs Cell line)		F(4,36) = 278.3, p -value < 0.0001	F(4,36) = 116.4, p -value < 0.0001	F(4,36) = 429.9, p -value < 0.0001
One-way ANOVA EAE		F(2,12) = 1820, p -value < 0.0001	F(2,12) = 94.87 p -value < 0.0001	F(2,12) = 104.5 p -value < 0.0001
One-way ANOVA $R_f = 0.65$		F(2,12) = 995.2 p -value < 0.0001	F(2,12) = 124.5 p -value < 0.0001	F(2,12) = 8220 p -value < 0.0001
One-way ANOVA $R_f = 0.72$		F(2,12) = 1.631 p -value = 0.2362	F(2,12) = 41.11 p -value < 0.0001	F(2,12) = 943.4 p -value < 0.0001

The comparison of cytotoxicity between EAE and the $R_f = 0.72$ fraction was 3 times significantly higher in the CoN cell line ($t = 2.333$, $df = 8$; $p = 0.024$) and 1.8 times higher in the PC-3 cell line ($t = 3.881$, $df = 8$; $p = 0.0023$) but was not significant in the HT-29 cell line ($t = 0.4472$, $df = 8$; $p = 0.3333$). However, for MCF-7, the cytotoxic activity was 2.3 times significantly lower ($t = 5.657$, $df = 8$; $p = 0.0002$) in comparison with the total EAE. Because the main activities are associated with EAE, $R_f = 0.65$ and $R_f = 0.72$, we used them for the subsequent analysis.

3.5. Induction of Cell Apoptosis by Bioactive Compounds

Morphological changes were observed in all analyzed cell lines (CoN, HT-29, PC-3 and MCF-7) after the treatment with the EAE and with the $R_f = 0.65$ and the $R_f = 0.72$ fractions (Figure 2). Untreated cells (controls) appeared as normal, angular and spindle-shaped, whereas prominent changes were observed in cells after 24 h of exposure to the extracts, adopting a spherical shape that tended to increase the aggregation distribution, indicating that cells appeared to have improved intercellular adhesion (mainly for $R_f = 0.72$), nuclear margination, nuclear fragmentation, chromatin condensation, secondary necrotic cells, apoptotic bodies and late apoptotic cells. These results were confirmed when cells were labeled with Hoechst 33342 (Figure 3E–H). Cell shrinkage with lesser cytoplasm mass was also observed (indicated by arrows; Figure 3), with their number varying accordingly to the cancer cell line (Figure 3). The most prominent effect was observed in the HT-29 cell line, whereas the PC-3 cell line was the least sensitive to the extracts (Figures 2 and 3; Table 1).

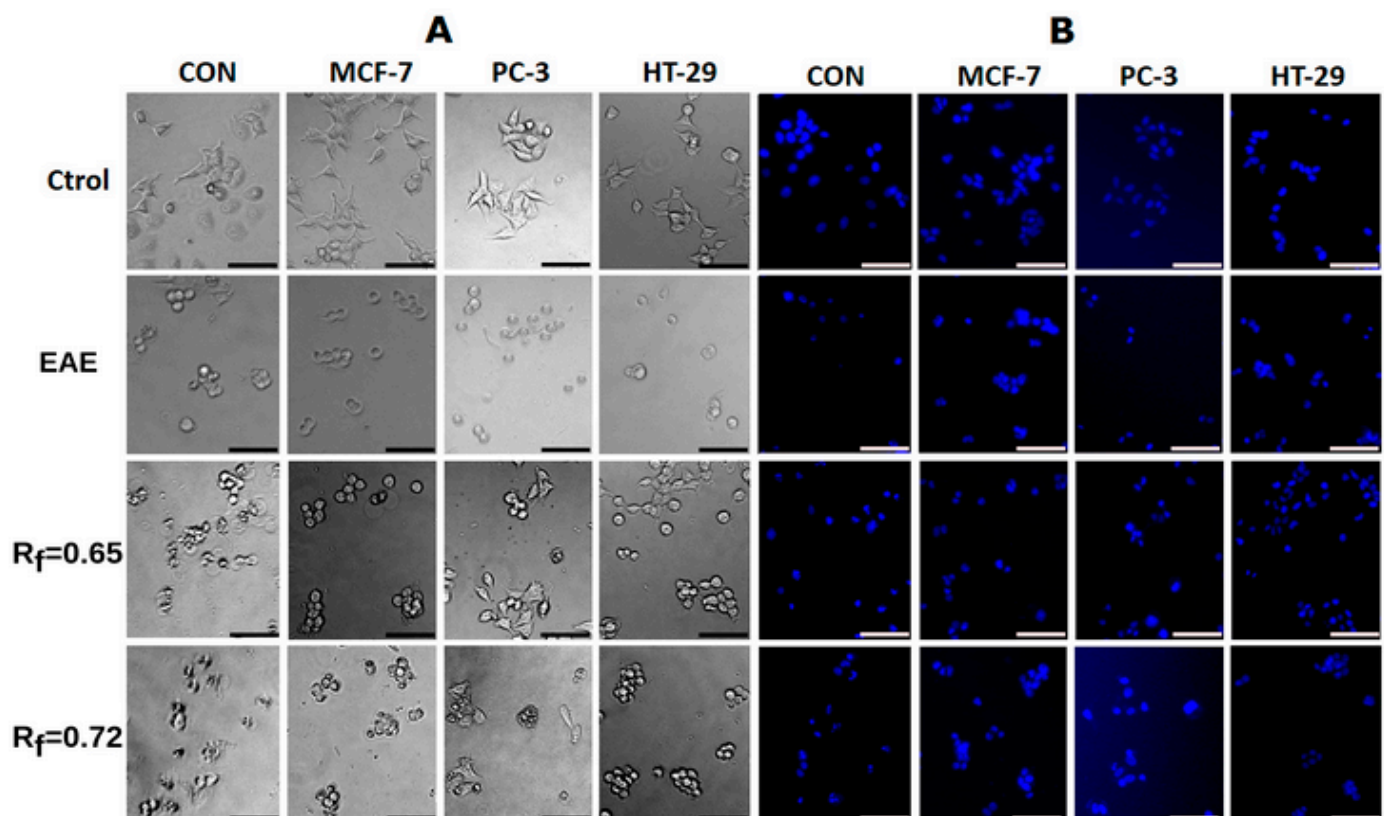


Figure 2. Cell morphology of different cancer cell lines (MCF-7, PC-3 and HT-29) unlabeled (A) or labeled with Hoechst 33342 (B) after treatment with EAE, $R_f = 0.65$ and $R_f = 0.72$ fractions. When cells were labelled with Hoechst 33342, it was possible to observe evidence of DNA condensation and the presence of apoptotic bodies, showing characteristic cells undergoing apoptosis. Scale bars: 50 μm .

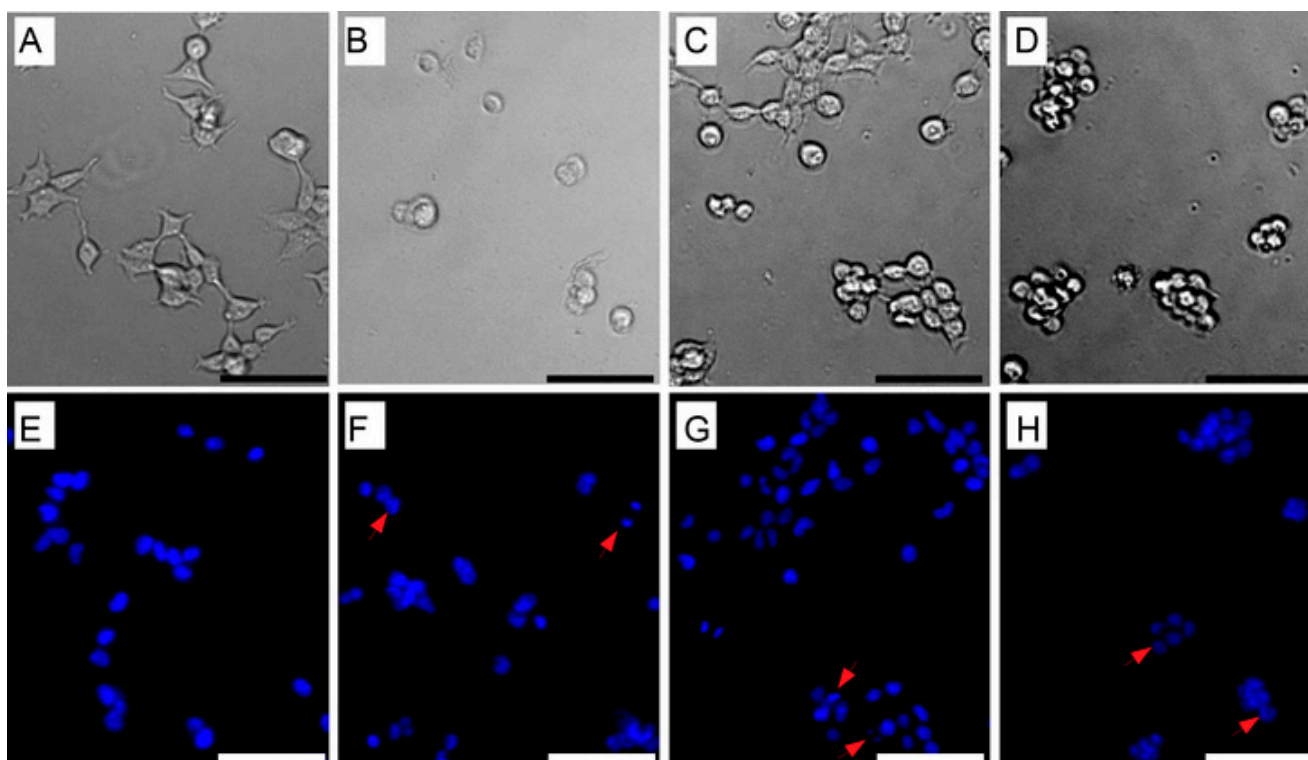


Figure 3. Morphological evidence of HT-29 cell apoptosis after 24 h of exposure with *Streptomyces* EAE, $R_f = 0.65$ and $R_f = 0.72$ fractions. (A–D) Morphology of unlabeled cells; (E–H) Chromatin condensation in the HT-29 cell line. Images were obtained with an inverted phase-contrast microscope (200 \times): (A) Control HT-29 cells; (B) HT-29 cells treated with EAE; (C) HT-29 cells treated with $R_f = 0.65$; (D) HT-29 cells treated with $R_f = 0.72$; (E–H) Cells treated with extracts or fractions stained with Hoechst 33342 (400 \times). Representative photographs of nuclear morphological changes: (E) Control HT-29 cells, (F) HT-29 cells treated with EAE; (G) HT-29 cells treated with $R_f = 0.65$; (H) HT-29 cells treated with $R_f = 0.72$. Scale bars: 50 μ m.

3.6. Reduction in Mitochondrial Membrane Potential (MMP) by Bioactive Compounds

Cancer cell lines treated with the EAE and the $R_f = 0.65$ and $R_f = 0.72$ fractions from *S. fildesensis* INACH3013 showed a reduction in the MMP. This reduction was statistically significant ($p < 0.0001$) for the CoN, PC-3 and HT-29 cells lines (Table 2). Moreover, the MMP reduction varied significantly according to the exposure time and the utilized fraction (two-way ANOVA using all cell lines—EAE: $F(4,36) = 1226.11$, $p < 0.0001$; $R_f = 0.65$: $F(4,36) = 1296.27$, $p < 0.0001$; $R_f = 0.72$: $F(4,36) = 322.53$, $p < 0.0001$).

In the case of CoN cells, the MMP decreased significantly when increasing the time of exposure to EAE and $R_f = 0.65$ (one-way ANOVA—EAE: $p < 0.0001$; $R_f = 0.65$: $p < 0.0001$). The percentage of labeled cells labeled reached a maximum value of 32% at 48 h after treatment with EAE. The treatment of $R_f = 0.65$ decreased the MMP percentage significantly over time, reaching 15% at 48 h. The $R_f = 0.72$ fraction exerted a significant reduction in MMP in CoN cells (two-way ANOVA, $p < 0.0001$), reaching 21% at 12 h, with no significant changes over time (24 h, 48 h; one-way ANOVA, $p = 0.2362$). For the PC3 cell line, the maximal reduction was observed at 48 h when exposed to both the EAE and $R_f = 0.65$ (46.9% and 91.3%, respectively).

Conversely, there was a decrease in the percentage of reduction when PC3 cells were treated with the $R_f = 0.72$ extract over time. A similar trend was observed in the HT-29 cells, with a maximal potential reduction (98.8%) when cells were treated with the $R_f = 0.65$ extract for 48 h.

For the PC3 cells, treatment with EAE induced a decrease in the MMP, reaching a level of 34% and maintaining this level for 12–24 h. Then, this effect tended to be reversed, increasing significantly to 47% at 48 h (one-way ANOVA, $p < 0.0001$).

In a similar way, the $R_f = 0.65$ fraction reached 36% at 12 h; then, this result increased significantly from 81% to 91% at 24 and 48 h, respectively (one-way ANOVA, $p < 0.0001$). The fraction $R_f = 0.72$ reached MMP values of 44% and 43% at 12 and 24 h, respectively. Moreover, the $R_f = 0.72$ fraction decreased significantly to 36% at 48 h (one-way ANOVA, $p < 0.0001$).

After treatment with EAE extract, the percentage of HT-29 cells marked with rhodamine 123 reached 26% at 12 h. However, this result tended to be reversed, significantly increasing the percentage of cells marked to 82% and 99% at 24 h and 48 h, respectively. Contrary to treatment EAE and $R_f = 0.65$, in cells treated with $R_f = 0.72$, it was possible to first observe a decrease in MMP that corresponded to 37.5% after 12 h and then a new significant decrease of 28% and 24% at 24 h and 48 h, respectively (one-way ANOVA, $p < 0.0001$).

3.7. Caspase Induction in CoN, PC-3 and HT-29 Cancer Cell Lines

As shown in Table 3, treatment with the extracts exerted a significant induction in the activity of caspases in all analyzed cell lines but mainly in the HT-29 cell line. EAE was the most effective treatment in inducing caspase activity in HT-29 cells, with a fold caspase induction of 1.6. $R_f = 0.65$ was the only effective extract against the PC-3 and HT-29 cell lines, with a fold caspase induction of 1.3. The three fractions did not induce the caspase activity in CoN cells.

Table 3. Caspase induction in CoN, PC-3 and HT-29 cell lines. Time induction values and fold increases relative to the control after cell treatment for 48 h with total ethyl acetate extracts (EAE), $R_f = 0.65$ fraction and $R_f = 0.72$ fraction, as described in Materials and Methods.

Treatments	Fold Induction of Caspases		
	Cell Lines		
	CoN	PC-3	HT-29
EAE	0.0	0.1	1.6
$R_f = 0.65$	0.3	1.3	1.3
$R_f = 0.72$	0.5	0.1	1.3

4. Discussion

Species of the genus *Streptomyces* have been responsible for producing two-thirds of all therapeutic bioactive metabolites [4], which, in many cases, have shown high toxicity, being effective on Gram (+), Gram (−) and human pathogenic fungi [2,6,7,14]. The same toxic effect has been observed on different human cancer cell lines [5,9,11,13]. This broad spectrum of action is an important characteristic that must be met by metabolites that are synthesized as chemical defenses [4].

The thermal degradation of bioactive compounds has been described as an important feature related to their antimicrobial activity [29]. Here, we show that EAE and bioactive TLC bands ($R_f = 0.65$ and $R_f = 0.72$) from the INACH3013 strain are thermostable at 100 °C for 30 min. Despite thermal treatment, EAE and bioactive TLC bands showed a significant reduction in antimicrobial activity after prolonged exposure (Figure 1). Additionally, the chemical characterization of those compounds in the two TLC spots with sulfuric acid, ninhydrin and the UV–visible spectra of both HPLC purified fractions showed that the absorbance ratio of 240 nm to that at 445 nm was between 1.30 and 1.50 when observed between 220 and 500 nm (Figure 1B). According to this and considering that $R_f = 0.65$ used the same migration of actinomycin D as the control, it is possible to suggest that both compounds belong to the actinomycin class due to the color and UV–visible spectra, as described previously by JH Lee and coworkers [30,31]. On the other hand, the FTIR

spectrum obtained for the compound was highly consistent with the spectrum obtained in the case of actinomycin D (Figures S1 and 1C). When comparing the spectra, it was possible to observe a marked profile with only slight differences in the area of the bands of the most relevant functional groups, showing that this compound would belong to the actinomycin family. In a broad sense, the signals corresponding to the carbonyls associated with the structures (ester, ketone and amide) could be clearly distinguished in the area of 1600 to 1700 cm^{-1} . In the region of 2900 to 3500 cm^{-1} , we expected to observe bands associated with the vibrations of the aliphatic and aromatic C-H bonds; however, the sample contained traces of water that masked the bands present in that region due to the great intensity of the O-H vibration of water. Actinomycin corresponds to a chromopeptide composed of a heterocyclic chromophore and two cyclic pentapeptide lactone rings with potent antimicrobial and antitumor activity [32,33]. In agreement with previous references, cyclic peptides are well recognized due to their high resistance to thermal degradation [34], as demonstrated by actinomycin D when exposed to 80 °C for a prolonged period (180 min) [35,36].

Genome sequencing has allowed for the generation of large databases with sequences of over 300 *Streptomyces* spp. An analysis of these data showed that *Streptomyces* species express only a fraction of their biosynthetic genes under laboratory growth conditions [37].

The antiSMASH analysis has been used as an indirect approach to confirm the presence of the actinomycin cluster. This analysis reveals differences in terms of the number of BGCs but also in the functional assignment of the genes between both *S. fildesensis* INACH3013 (32 BGCs) and its sister strain, *S. fildesensis* So13.3 (29 BGCs). However, these differences may obey the incomplete genome of INACH3013, which also generates differences in the putative BGC assignment by antiSMASH, because most of the BGCs detected in INACH3013 are represented in the edge of the contigs of the partial genome (Table S1).

Different strains of the same *Streptomyces* species usually harbor between 19 and 28 putative secondary metabolite genes clusters, with at least one unique strain-specific biosynthetic gene cluster [37]. INACH3013 and SO13.3 correspond to sister strains, with a difference in % G+C of 0.02, an ANIb of 99%, an ANIm of 99.65 and an iSSDH of 96.50%. BLAST and synteny analysis between both strains revealed that actinomycin D is present in both *Streptomyces fildesensis* strains. Actinomycin V (structural analog of actinomycin D) was recently reported as the main compound produced by the *Streptomyces* strain (CMAA-1653, GenBank MH241012) and is also present in the So13.3 strain [7,8], both related to *S. fildesensis*. It is well known that different strains of the same species of streptomycetes can share common putative BGCs, with at least one unique strain-specific biosynthetic gene cluster as a result of the presence or absence of genes or mutations that result in distinct final structures of metabolites [37,38]. The partial chemical characterization and thermal stability features, in combination with the BCG analysis on the draft genome, reinforce the production of actinomycin-like compounds by the INACH3013 strain.

In this study, the cytotoxicity of CFS, EAE and two purified fractions, $R_f = 0.65$ and $R_f = 0.72$, were evaluated via in vitro experiments by using frequently diagnosed human colorectal adenocarcinoma (HT-29), human breast carcinoma (MCF-7), human prostatic adenocarcinoma (PC-3) and the non-tumor CoN cell line. The results indicate different degrees of cytotoxicity on tumor cell lines (Table 1), being similar and non-selective for all cell lines. Considering previous studies on *Streptomyces* [8,39], it is possible to confirm that the range of the cytotoxic effects of the extracts from the INACH3013 strain were similar for all cell lines. Both the EAE and the $R_f = 0.72$ fractions showed high toxicity against the HT-29 cell line, with EC_{50} values of 0.1 and 0.09 $\mu\text{g}/\text{mL}$, respectively, and the CFS extract had an EC_{50} value of 13.42 $\mu\text{g}/\text{mL}$. These results correspond to the obtained range of values of EC_{50} when colorectal carcinoma cell lines (HCT-116) were exposed to cell extracts from the genus *Streptomyces*, ranging from 71.0 to 0.076 $\mu\text{g}/\text{mL}$ [40]. Similar values of EC_{50} were found in the HT-29 and MCF-7 cell lines when exposed to actinomycin V, produced by closely related strains (99.26% of 16S rRNA gene similarity to *S. fildesensis*) [8,39]. In fact, it has been shown that actinomycin V presents higher toxicity than actinomycin D [39,41], suggesting

that $R_f = 0.72$ could correspond to actinomycin V, as previously described for the related *S. fildesensis* strain [8]. However, more detailed analyses are needed to elucidate functional groups and chemical structures because it is well known that several *Streptomyces* species synthesize actinomycins D, V and X2 or X2 and D simultaneously [42–44].

With respect to the induction of apoptosis, it is known that programmed cell death plays a key role in the survival of normal and cancerous cells [45]. In cancer cells, all pro-apoptotic stimulations are inhibited to ensure the survival and proliferation of the tumor [46]. Programmed cell death is an important target when evaluating the potential of new metabolites or anticancer extracts. Apoptosis implies morphological and biochemical changes [45] at the morphological level, including cell shrinkage, improved intercellular adhesion, nuclear condensation, nuclear fragmentation and the loss of adhesion to the extracellular matrix (Figures 2 and 3). Cellular contraction and the loss of adhesion were evident under photonic microscopy, whereas under fluorescence microscopy, after applying nuclear fluorescent dye Hoechst 33342, we observed the condensation of the nucleus and the formation of apoptotic bodies (Figure 3). These changes have been reported in other studies when cells were exposed to actinomycin compounds [39,41]. Actinomycin has been described to be responsible for the down-regulation of the mRNA expression levels of N-cadherin and vimentin, inhibiting the epithelial–mesenchymal transition and consecutively suppressing the migration and invasion of cancer cells by morphological changes [39].

Actinomycin has been reported as a potent inducer of apoptosis in different cells in vitro and in vivo assays. Moreover, different pathways have been described involving a p53-dependent or independent fashion and a tumor-necrosis-factor-related apoptosis-inducing ligand (TRAIL) [10,11,41,47]. At the molecular level, apoptosis can be induced through a signaling pathway associated with the permeability of the mitochondria membrane (intrinsic pathway) that releases pro-apoptotic proteases to the cytosol that activate the caspases, which are ultimately responsible for carrying out apoptosis [48]. In our study, the EAE and the $R_f = 0.65$ and $R_f = 0.72$ extracts clearly affected the MMP and also induced the activation of caspases at different degrees (Table 2). However, only the $R_f = 0.65$ fraction triggered the irreversible induction of apoptosis in the PC-3 and HT-29 cell lines (Table 2), with both having higher values of caspase induction (Table 3). The results suggest that the mechanism of cell apoptosis is similar to what has been reported for the action mode of actinomycin D in human neuroblastoma SH-SY5Y cells, decreasing mitochondrial transmembrane potential and enhancing apoptosis through caspase-dependent and -independent manners [47].

Our findings suggest that the possible mechanism of cell death in MCF-7, PC-3 and HT-29, and in the non-tumor cell line CoN, is associated with this intrinsic pathway linked to the mitochondrion and the activation of caspases triggered by actinomycin.

The current information about the actinomycin biosynthetic gene cluster similarity analysis (89%) of *S. fildesensis* suggests the potential presence of new structurally related molecules, and further analysis must be conducted in order to elucidate its chemical structures and relationships with the antitumoral action mechanism to investigate its medicinal properties. Moreover, it is important to continue research to explore if this intrinsic pathway linked to the mitochondrion and the activation of caspases triggered by those actinomycins is operating in other cancer cell lines.

5. Conclusions

As expected, for several *Streptomyces* strains, the Antarctic *S. fildesensis* INACH3013 is able to produce two compounds ($R_f = 0.72$ and $R_f = 0.65$) that belong to the actinomycin family, as confirmed by functional groups via FTIR and chromatography analysis.

Despite both compounds displaying remarkable antimicrobial and cytotoxic activity against human cell lines, the activity of compound $R_f = 0.72$ was higher in comparison to the compound $R_f = 0.65$ (related to actinomycin D). Further research using modern techniques such as nuclear magnetic resonance (NMR) could bring new and unambiguous information about its chemical structure.

Actinomycin compounds are well known for their use as anticancer drugs and their antimicrobial activity. The present work confirms both the antimicrobial and cytotoxic activity (apoptosis mediated by caspase activation) of actinomycin compounds produced by *S. fildesensis* INACH3013, which is relevant not only for the discovery of novel bioactive compounds but also as a new source of actinomycin compounds to address the needs of industrial pharmaceuticals.

Supplementary Materials: The following supporting information can be downloaded at <https://www.mdpi.com/article/10.3390/fermentation9020129/s1>: Figure S1: (a) Two-Dimensional Thin layer chromatography of EAE plus actinomycin—D (standard compound); 2D-TLC plate was visualized using 10% sulphuric acid in methanol solution and heated; Ethyl acetate:methanol (9:1, *v/v*) used as the mobile solvent in 1D-TLC and Ethyl acetate:methanol (8:2, *v/v*) for 2D-TLC. (b) Standard FTIR spectra of actinomycin with 20 and 40 factor dilution in KBr (red) and standard FTIR spectrum of actinomycin D (green). (c) Comparison of the FTIR spectrum (4000–400 cm^{-1}) of purified bands of R_f 0.65 and R_f 0.72; Table S1: Biosynthetic gene clusters identified in *Streptomyces fildesensis* INACH3013 genome. Biosynthetic gene clusters (% proportion of gene similarity) were determined as indicated in Methods; NRPS, non ribosomal synthesized peptide; RIPP-like, Other unspecified ribosomally synthesized and post-translationally modified peptides; NAPAA, non-alpha poly-amino acids like e-Polylysine; T1PKS, Type I polyketide synthase; T2PKS, Type II polyketide synthase; T3PKS, Type III polyketide synthase; LAP, Linear azol (in)e-containing peptides; CDPS, tRNA-dependent cyclodipeptide synthases).

Author Contributions: Conceptualization, D.A.-B., R.O. and P.L.; Formal analysis, C.H.-C. and N.F.-V.; Funding acquisition, R.O., D.A.-B., C.M.V.L.W. and P.L.; Investigation, D.A.-B.; Methodology, D.A.-B.; FTIR analysis, P.A.P.; Project administration, P.L.; Supervision, P.L.; Validation, C.H.-C. and J.M.P.-D.; Visualization, N.F.-V.; Writing—original draft preparation, D.A.-B., R.O., C.H.-C. and P.L.; Writing—review and editing, R.O., C.M.V.L.W., J.M.P.-D., C.P., H.F. and P.L. All authors have read and agreed to the published version of the manuscript.

Funding: This research was funded by Instituto Antartico Chileno (INACH), grant numbers MG_05–14 and N° RT_20–19. This work was also partially supported by Fondecyt Iniciación grant N° 11190754 (National Agency of Research and Development, ANID) and by grants ATA N° 2095 and ATA N° 20992 of the Ministry of Education of Chile, VRII-No1308 project Iniciación de la Investigación de Nuevos Investigadores de la Universidad de Antofagasta, Chile, Agencia Nacional de Investigación y Desarrollo (ANID) - CLAP R20F0008 and Yayasan Penyelidikan Antartika Sultan Mizan (YPASM) (UMS code LPS2110).

Institutional Review Board Statement: Not applicable.

Informed Consent Statement: Not applicable.

Data Availability Statement: Not applicable.

Acknowledgments: The authors wish to thank the Laboratory of Cancer from the University of Valparaíso and INACH (Chilean Antarctic Institute) through the Support Program for Postgraduate Thesis, and Yayasan Penyelidikan Antartika Sultan Mizan (YPASM), Malaysia.

Conflicts of Interest: The authors declare no conflict of interest.

References

1. Siegel, R.L.; Miller, K.D.; Jemal, A. Cancer statistics, 2020. *CA Cancer J. Clin.* **2020**, *70*, 7–30. [[CrossRef](#)]
2. Genilloud, O. Actinomycetes: Still a source of novel antibiotics. *Nat. Prod. Rep.* **2017**, *34*, 1203–1232. [[CrossRef](#)]
3. Newman, D.J.; Cragg, G.M. Natural Products as Sources of New Drugs over the Nearly Four Decades from 01/1981 to 09/2019. *J. Nat. Prod.* **2020**, *83*, 770–803. [[CrossRef](#)]
4. Singh, B.P.; Rateb, M.E.; Rodriguez-Couto, S.; Polizeli, M.D.L.T.D.M.; Li, W.J. Microbial secondary metabolites, Recent developments and technological challenges. *Front. Microbiol.* **2019**, *10*, 914. [[CrossRef](#)]
5. Sivalingam, P.; Hong, K.; Pote, J.; Prabakar, K. Extreme environment *Streptomyces*, potential sources for new antibacterial and anticancer drug leads? *Int. J. Microbiol.* **2019**, 5283948. [[CrossRef](#)] [[PubMed](#)]
6. Lavin, P.L.; Yong, S.T.; Wong, C.M.; De Stefano, M. Isolation and characterization of Antarctic psychrotroph *Streptomyces* sp strain INACH3013. *Antarct. Sci.* **2016**, *28*, 433–442. [[CrossRef](#)]

7. Núñez-Montero, K.; Lamilla, C.; Abanto, M.; Maruyama, F.; Jorquera, M.A.; Santos, A. Antarctic *Streptomyces fildesensis* So13.3 strain as a promising source for antimicrobials discovery. *Sci. Rep.* **2019**, *9*, 7488. [CrossRef]
8. Silva, L.J.; Crevelin, E.J.; Souza, D.T.; Lacerda-Júnior, G.V.; de Oliveira, V.M.; Ruiz, A.L.T.G.; Rosa, L.H.; Morales, L.A.B.; Melo, I.S. Actinobacteria from Antarctica as a source for anticancer discovery. *Sci. Rep.* **2020**, *10*, 13870. [CrossRef]
9. Cai, W.; Wang, X.; Elshahawi, S.I.; Ponomareva, L.V.; Liu, X.; McErlean, M.R.; Cui, Z.; Arlinghaus, A.L.; Thorson, J.S.; Van Lanen, S.G. Antibacterial and Cytotoxic Actinomycins Y6–Y9 and Zp from *Streptomyces* sp. Strain Gö–GS12. *J. Nat. Prod.* **2016**, *79*, 2731–2739. [CrossRef]
10. Yang, K.; Yang, J.; Yi, J. Nucleolar Stress: Hallmarks, sensing mechanism and diseases. *Cell Stress* **2018**, *2*, 125. [CrossRef]
11. Gionfriddo, I.; Brunetti, L.; Mezzasoma, F.; Milano, F.; Cardinali, V.; Ranieri, R.; Venanzi, A.; Pierangeli, S.; Vetro, C.; Spinozzi, G.; et al. Dactinomycin induces complete remission associated with nucleolar stress response in relapsed/refractory NPM1-mutated AML. *Leukemia* **2021**, *35*, 2552–2562. [CrossRef]
12. Atlas, R.M. *Handbook of Microbiological Media*, 4th ed.; CRC Press: Boca Raton, FL, USA, 2010.
13. Farida, Y.; Widada, J.; Meiyanto, E. Combination methods for screening marine actinomycetes producing potential compounds as anticancer. *Indones. J. Biotechnol.* **2007**, *12*, 988–997. [CrossRef]
14. Gopikrishnan, V.; Radhakrishnan, M.; Shanmugasundaram, T.; Ramakodi, M.P.; Balagurunathan, R. Isolation, characterisation and identification of antibiofouling metabolite from mangrove derived *Streptomyces sampsonii* PM33. *Sci Rep.* **2019**, *9*, 12975. [CrossRef]
15. Blin, K.; Shaw, S.; Steinke, K.; Villebro, R.; Ziemert, N.; Lee, S.Y.; Medema, M.H.; Weber, T. AntiSMASH 5.0, updates to the secondary metabolite genome mining pipeline. *Nucleic Acids Res.* **2019**, *47*, W81–W87. [CrossRef]
16. Richter, M.; Rosselló-Móra, R.; Glöckner, F.O.; Peplies, J. JSpeciesWS, a web server for prokaryotic species circumscription based on pairwise genome comparison. *Bioinformatics* **2015**, *32*, 929–931. [CrossRef]
17. Meier-Kolthoff, J.P.; Auch, A.F.; Klenk, H.P.; Göker, M. Genome sequence-based species delimitation with confidence intervals and improved distance functions. *BMC Bioinform.* **2013**, *14*, 60. [CrossRef]
18. Lavin, P.; Henríquez-Castillo, C.; Yong, S.T.; Valenzuela-Heredia, D.; Osés, R.; Frez, K.; Borba, M.P.; Purcarea, C.; Wong, C.M.V.L. Draft Genome Sequence of Antarctic Psychrotroph *Streptomyces fildesensis* Strain INACH3013, Isolated from King George Island Soil. *Microbiol. Resour. Announc.* **2021**, *10*, e01453-20. [CrossRef]
19. Vichai, V.; Kirtikara, K. Sulforhodamine B colorimetric assay for cytotoxicity screening. *Nat. Protoc.* **2006**, *1*, 1112. [CrossRef]
20. Zhivotosky, B.; Orrenius, S. Assessment of apoptosis and necrosis by DNA fragmentation and morphological criteria. *Curr Protoc. Cell Biol.* **2001**, *12*, 18–23. [CrossRef]
21. Crowley, L.C.; Marfell, B.J.; Waterhouse, N.J. Analyzing Cell Death by Nuclear Staining with Hoechst 33342. *Cold Spring Harb. Protoc.* **2016**, *9*, 778–781. [CrossRef]
22. Pozarowski, P.; Huang, X.; Halicka, D.H.; Lee, B.; Johnson, G.; Darzynkiewicz, Z. Interactions of fluorochrome-labeled caspase inhibitors with apoptotic cells, A caution in data interpretation. *Cytom. A* **2003**, *55*, 50–60. [CrossRef] [PubMed]
23. Rouet-Benzineb, P.; Rouyer-Fessard, C.; Jarry, A.; Avondo, V.; Pouzet, C.; Yanagisawa, M.; Laboisie, C.; Laburthe, M.; Voisin, T. Orexins acting at native OX1. receptor in colon cancer and neuroblastoma cells or at recombinant OX1. receptor suppress cell growth by inducing apoptosis. *J. Biol. Chem.* **2004**, *279*, 45875–45886. [CrossRef] [PubMed]
24. R Core Team. *R, A Language and Environment for Statistical Computing*; R Foundation for Statistical Computing: Vienna, Austria, 2020. Available online: <https://www.R-project.org/> (accessed on 30 April 2021).
25. Wickham, H.; Averick, M.; Bryan, J.; Chang, W.; McGowan, L.D.A.; François, R. Welcome to the Tidyverse. *J. Open Source Softw.* **2019**, *4*, 1686. [CrossRef]
26. Hadley, W.; Romain, F.; Lione, I.H.; Kirill, M. dplyr, A Grammar of Data Manipulation. R Package Version 1.0.2. 2020. Available online: <https://CRAN.R-project.org/package=dplyr> (accessed on 30 April 2021).
27. Ritz, C.; Baty, F.; Streibig, J.C.; Gerhard, D. Dose-Response Analysis Using R. *PLoS ONE* **2015**, *10*, e0146021. [CrossRef]
28. Wickham, H. *ggplot2, Elegant Graphics for Data Analysis*; Springer-Verlag: New York, NY, USA, 2016; p. 260.
29. Hsieh, M.K.; Shyu, C.L.; Liao, J.W.; Franje, C.A.; Huang, Y.J.; Chang, S.K.; Shih, P.Y.; Chou, C. Correlation analysis of heat stability of veterinary antibiotics by structural degradation, changes in antimicrobial activity and genotoxicity. *Vet. Med.* **2011**, *56*, 274–285. [CrossRef]
30. Lee, J.H.; Kim, Y.G.; Lee, K.; Kim, C.J.; Park, D.J.; Ju, Y. *Streptomyces*-derived actinomycin D inhibits biofilm formation by *Staphylococcus aureus* and its hemolytic activity. *Biofouling* **2016**, *32*, 45–56. [CrossRef]
31. World Health Organization. *The International Pharmacopoeia*, 9th ed.; World Health Organization: Geneva, Switzerland, 2019. Available online: <https://apps.who.int/phint/pdf/b/6.1.111.Dactinomycin-Dactinomycinum.pdf> (accessed on 30 April 2021).
32. Hollstein, U. Actinomycin. Chemistry and mechanism of action. *Chem. Rev.* **1974**, *74*, 625–652. [CrossRef]
33. Węglarz-Tomczak, E.; Talma, M.; Giurg, M.; Westerhoff, H.V.; Janowski, R.; Mucha, A. Neutral metalloaminopeptidases APN and MetAP2 as newly discovered anticancer molecular targets of actinomycin D and its simple analogs. *Oncotarget* **2018**, *9*, 29365. [CrossRef]
34. Sable, R.; Durek, T.; Taneja, V.; Craik, D.J.; Pallerla, S.; Gauthier, T.; Jois, S. Constrained cyclic peptides as immunomodulatory inhibitors of the CD2, CD58 protein–protein interaction. *ACS Chem. Biol.* **2016**, *11*, 2366–2374. [CrossRef]
35. Crevar, G.E.; Slotnick, I.J. A note on the stability of actinomycin D. *J. Pharm. Pharmacol.* **1964**, *16*, 429–432. [CrossRef]

36. Bini, E.; Dikshit, V.; Dirksen, K.; Drozda, M.; Blum, P. Stability of mRNA in the hyperthermophilic archaeon *Sulfolobus solfataricus*. *RNA* **2002**, *8*, 1129–1136. [[CrossRef](#)] [[PubMed](#)]
37. Seipke, R.F. Strain-Level Diversity of Secondary Metabolism in *Streptomyces albus*. *PLoS ONE* **2015**, *10*, e0116457. [[CrossRef](#)] [[PubMed](#)]
38. Nicault, M.; Tidjani, A.R.; Gauthier, A.; Dumarcay, S.; Gelhaye, E.; Bontemps, C.; Leblond, P. Mining the biosynthetic potential for specialized metabolism of a *Streptomyces* soil community. *Antibiotics* **2020**, *9*, 271. [[CrossRef](#)] [[PubMed](#)]
39. Lin, S.; Zhang, C.; Liu, F.; Ma, J.; Jia, F.; Han, Z. Actinomycin V inhibits migration and invasion via suppressing snail/sluc-mediated epithelial-mesenchymal transition progression in human breast cancer MDA-MB-231 cells in vitro. *Mar. Drugs* **2019**, *17*, 305. [[CrossRef](#)] [[PubMed](#)]
40. Becerril-Espinosa, A.; Guerra-Rivas, G.; Ayala-Sánchez, N.; Soria-Mercado, I.E. Antitumor activity of actinobacteria isolated in marine sediment from Todos Santos Bay Baja California Mexico. *Rev. Biol. Mar. Oceanogr.* **2012**, *47*, 317–325. [[CrossRef](#)]
41. Lin, S.Q.; Jia, F.J.; Zhang, C.Y.; Liu, F.Y.; Ma, J.H.; Han, Z.; Xie, W.-D.; Li, X. Actinomycin V suppresses human non-small-cell lung carcinoma A549 cells by inducing G2/M phase arrest and apoptosis via the p53-dependent pathway. *Mar. Drugs* **2019**, *17*, 572. [[CrossRef](#)] [[PubMed](#)]
42. Liu, M.; Jia, Y.; Xie, Y.; Zhang, C.; Ma, J.; Sun, C.; Ju, J. Identification of the actinomycin D biosynthetic pathway from marine-derived *Streptomyces costaricanus* SCSIO ZS0073. *Mar. Drugs* **2019**, *17*, 240. [[CrossRef](#)]
43. Qureshi, K.A.; Bholay, A.D.; Rai, P.K.; Mohammed, H.A.; Khan, R.A.; Azam, F.; Jaremko, M.; Emwas, A.; Stefanowicz, P.; Waliczek, M.; et al. Isolation; characterization; anti-MRSA evaluation; and in-silico multi-target anti-microbial validations of actinomycin X2 and actinomycin D produced by novel *Streptomyces smyrnaeus* UKAQ_23. *Sci. Rep.* **2021**, *11*, 14539. [[CrossRef](#)]
44. Sharma, M.; Manhas, R.K. Purification and characterization of actinomycins from *Streptomyces* strain M7 active against methicillin resistant *Staphylococcus aureus* and vancomycin resistant *Enterococcus*. *BMC Microbiol.* **2019**, *19*, 44. [[CrossRef](#)]
45. Ouyang, L.; Shi, Z.; Zhao, S.; Wang, F.T.; Zhou, T.T.; Liu, B.; Bao, J.K. Programmed cell death pathways in cancer, a review of apoptosis autophagy and programmed necrosis. *Cell Prolif.* **2012**, *45*, 487–498. [[CrossRef](#)]
46. Fernald, K.; Kurokawa, M. Evading apoptosis in cancer. *Trends Cell Biol.* **2013**, *23*, 620–633. [[CrossRef](#)] [[PubMed](#)]
47. Wang, M.J.; Liu, S.; Liu, Y.; Zheng, D. Actinomycin D enhances TRAIL-induced caspase-dependent and-independent apoptosis in SH-SY5Y neuroblastoma cells. *Neurosci. Res.* **2007**, *59*, 40–46. [[CrossRef](#)] [[PubMed](#)]
48. Eum, K.H.; Lee, M. Crosstalk between autophagy and apoptosis in the regulation of paclitaxel-induced cell death in v-Ha-ras-transformed fibroblasts. *Mol. Cell Biochem.* **2011**, *348*, 61–68. [[CrossRef](#)] [[PubMed](#)]

Disclaimer/Publisher’s Note: The statements, opinions and data contained in all publications are solely those of the individual author(s) and contributor(s) and not of MDPI and/or the editor(s). MDPI and/or the editor(s) disclaim responsibility for any injury to people or property resulting from any ideas, methods, instructions or products referred to in the content.